

**Journal of  
Mechanics of  
Materials and Structures**

**DYNAMIC STIFFNESS VIBRATION ANALYSIS OF THICK SPHERICAL  
SHELL SEGMENTS WITH VARIABLE THICKNESS**

Elia Efraim and Moshe Eisenberger

**Volume 5, No. 5**

**May 2010**



**mathematical sciences publishers**

## DYNAMIC STIFFNESS VIBRATION ANALYSIS OF THICK SPHERICAL SHELL SEGMENTS WITH VARIABLE THICKNESS

ELIA EFRAIM AND MOSHE EISENBERGER

A dynamic stiffness method is presented for determining the free vibration frequencies and mode shapes of thick spherical shell segments with variable thickness and different boundary conditions. The analysis uses the equations of the two-dimensional theory of elasticity, in which the effects of both transverse shear stresses and rotary inertia are accounted for. The displacement components are taken to be sinusoidal in time, periodic in the circumferential direction, constant through the thickness, and solved exactly in the meridional direction using the exact element method. The shape functions are derived from the exact solutions for the system of the differential equation of motion with variable coefficients. The dynamic stiffness matrix is derived from the exact shape functions and their derivatives. High-precision numerical results are presented for thick spherical shell segments with constant or linearly varying thickness and for several combinations of boundary conditions. Comparison is made with results of published research and with two- and three-dimensional finite element analyses.

### 1. Introduction

Spherical shells are extensively used in civil, mechanical, aircraft, and naval structures. The free vibration of solid and hollow spheres has been a subject of study for more than a century. Historical reviews of the research into the vibrations of spherical shell are given in [Leissa 1973; Kang and Leissa 2000; Qatu 2002]. For segmented spherical shells very few studies can be found. Gautham and Ganesan [1992] used finite elements to study the free vibration analysis of open spherical shells, based on a thick (two-dimensional) shell theory. A thick shell finite element was derived and vibration frequencies were obtained for spherical caps with and without center cutout having simply supported or clamped boundary conditions. Lim et al. [1996] analyzed spherical shells with variable thickness using two-dimensional shell theory and the Ritz method, and the results were compared with finite element and experimental ones. For spherical shell segments based on three-dimensional analysis, Kang and Leissa [2000] used the Ritz method to obtain accurate frequencies for thick spherical shell segments of uniform or varying thickness. Their method does not yield exact solutions, but with proper use of displacement components in the form of algebraic polynomials, one is able to obtain frequency upper bounds, that are as close to the exact values as desired. Corrected results for the test cases in that paper appeared subsequently in [Kang and Leissa 2006].

In this paper the equations of motion for a thick spherical shell segment with variable thickness are derived. Then, these are solved for the dynamic stiffness matrix of the segment, and assembled for a complete structure.

---

*Keywords:* vibrations, thick shell, spherical shell, variable thickness, dynamic stiffness, exact element method.

Support given this research to the first author by the Technion – Israel Institute of Technology is gratefully acknowledged.

### 2. Equations of motion

The shell coordinates and shell parameters for axisymmetric spherical shells with thickness varying along the meridian are shown in [Figure 1](#), left, where  $\phi$  and  $\theta$  are spherical angle coordinates,  $z$  is thickness coordinate from middle surface,  $R_0$  is radius of curvatures of the middle surface of the shell in both meridian and circumferential directions and  $R_p(\phi)$  describes the perpendicular distance to the axis of revolution of the generating line. The location of the shell segment is defined by either the angle of the beginning of the shell  $\phi_b$ , or the angle of the end of the shell segment  $\phi_e$ , and the meridional dimension of the shell is defined by the opening angle  $\phi_0$ .

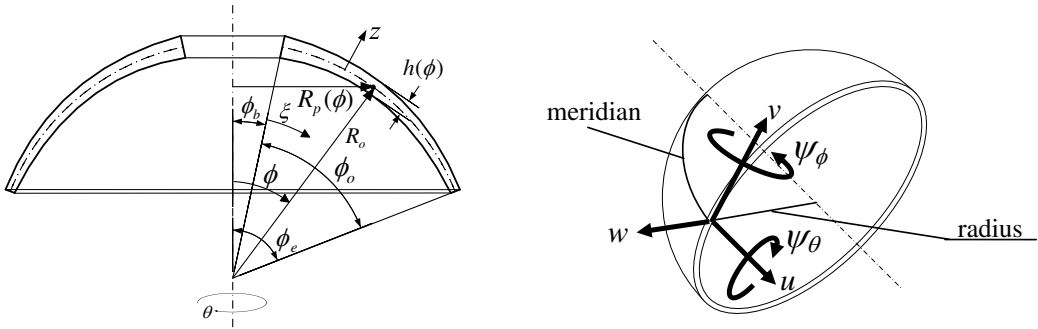


**Figure 1.** Left: geometry and coordinates of a spherical shell segment. Right: displacement field according to the thick shell theory.

The strain-displacement equations of the first order shear deformation shell theory of thick shells are obtained by satisfying the Kirchoff–Love hypothesis, such that normal to the shell mid-surface during deformation remain straight, and suffer no extension, but are not necessarily normal to the mid-surface after deformation. According to these assumptions the displacement of every point of the shell (see [Figure 1](#), right) may be expressed as

$$\begin{aligned} u(\phi, \theta, z, t) &= U_0(\phi, \theta, t) + z\Psi_\phi(\phi, \theta, t), \\ v(\phi, \theta, z, t) &= V_0(\phi, \theta, t) + z\Psi_\theta(\phi, \theta, t), \\ w(\phi, \theta, z, t) &= W_0(\phi, \theta, t) \end{aligned} \tag{1}$$

and the strain-displacement equations given in [\[Leissa and Chang 1996\]](#) for a general spherical shell become, for a spherical shell segment,

$$\begin{aligned} \epsilon_\phi &= \frac{\epsilon_{0\phi} + zk_\phi}{1 + z/R_0}, & \epsilon_\theta &= \frac{\epsilon_{0\theta} + zk_\theta}{1 + z/R_0}, \\ \gamma_{\phi\theta} &= \frac{\gamma_{0\phi\theta} + z\tau_{\phi\theta} + \gamma_{0\theta\phi} + z\tau_{\theta\phi}}{1 + z/R_0}, \\ \gamma_{\phi z} &= \frac{\gamma_{0\phi z}}{1 + z/R_0}, & \gamma_{\theta z} &= \frac{\gamma_{0\theta z}}{1 + z/R_0}, \end{aligned} \tag{2}$$

where we have denoted by  $\epsilon_{0..}$ ,  $\gamma_{0..}$  and  $k$ . the strains and curvatures of the middle surface of the shell, given by the expressions

$$\begin{aligned}
 \epsilon_{0\phi} &= \frac{1}{R_0} \frac{\partial U_0}{\partial \phi} + \frac{W_0}{R_0}, & \epsilon_{0\theta} &= \frac{1}{R_p} \frac{\partial V_0}{\partial \theta} + \frac{U_0}{R_0 R_p} \frac{\partial R_p}{\partial \phi} + \frac{W_0}{R_0}, \\
 k_\phi &= \frac{1}{R_0} \frac{\partial \Psi_\phi}{\partial \phi}, & k_\theta &= \frac{1}{R_p} \frac{\partial \Psi_\theta}{\partial \theta} + \frac{\Psi_\phi}{R_0 R_p} \frac{\partial R_p}{\partial \phi}, \\
 \gamma_{0\phi\theta} &= \frac{1}{A} \frac{\partial V_0}{\partial \phi}, & \gamma_{0\theta\phi} &= \frac{1}{R_p} \frac{\partial U_0}{\partial \theta} - \frac{V_0}{R_0 R_p} \frac{\partial R_p}{\partial \phi}, \\
 \gamma_{0\phi z} &= \frac{1}{R_0} \frac{\partial W_0}{\partial \phi} \frac{U_0}{R_0} + \Psi_\phi, & \gamma_{0\phi z} &= \frac{1}{R_p} \frac{\partial W_0}{\partial \theta} - \frac{V_0}{R_0} + \Psi_\theta.
 \end{aligned} \tag{3}$$

Substituting the shell parameters into the five equations of motion of general shells [Leissa and Chang 1996] using the relations for principle shell coordinates ( $\alpha_1 = \phi, \alpha_2 = \theta$ ), Lamé’s coefficients ( $A = R_0, B = R_p(\phi) = R_0 \sin \phi$ ) and radii of curvatures ( $R_1 = R_2 = R_0$ ) yields the five equilibrium equations for a spherical shell segment with variable thickness:

$$\left. \begin{aligned}
 &\frac{dR_p(\phi)}{d\phi} N_\phi(\phi, \theta) + R_p(\phi) \frac{\partial N_\phi(\phi, \theta)}{\partial \phi} + R_0 \frac{\partial N_{\theta\phi}(\phi, \theta)}{\partial \theta} - \frac{\partial R_p(\phi)}{\partial \phi} N_\theta(\phi, \theta) \\
 &\quad + R_0 R_p(\phi) Q_\phi(\phi, \theta) - R_p(\phi) (R_0 I_1(\phi) \ddot{U}_0(\phi, \theta, t) + 2I_3(\phi) \ddot{\Psi}_\phi(\phi, \theta, t)) = 0, \\
 &R_0 \frac{\partial N_\theta(\phi, \theta)}{\partial \theta} + \frac{dR_p(\phi)}{d\phi} N_{\phi\theta}(\phi, \theta) + R_p(\phi) \frac{\partial N_{\phi\theta}(\phi, \theta)}{\partial \phi} + \frac{dR_p(\phi)}{d\phi} N_{\theta\phi}(\phi, \theta) \\
 &\quad + R_p(\phi) Q_\theta(\phi, \theta) - R_p(\phi) (R_0 I_1(\phi) \ddot{V}_0(\phi, \theta, t) + 2I_3(\phi) \ddot{\Psi}_\theta(\phi, \theta, t)) = 0, \\
 &-R_p(\phi) N_\phi(\phi, \theta) - R_p(\phi) N_\theta(\phi, \theta) + \frac{\partial R_p(\phi)}{\partial \phi} Q_\phi(\phi, \theta) \\
 &\quad + R_p(\phi) \frac{\partial Q_\phi(\phi, \theta)}{\partial \phi} + R_0 \frac{\partial Q_\theta(\phi, \theta)}{\partial \theta} - R_0 R_p(\phi) I_1(\phi) \ddot{W}_0(\phi, \theta, t) = 0, \\
 &\frac{dR_p(\phi)}{d\phi} M_\phi(\phi, \theta) + R_p(\phi) \frac{\partial M_\phi(\phi, \theta)}{\partial \phi} + R_0 \frac{\partial M_{\theta\phi}(\phi, \theta)}{\partial \theta} - \frac{\partial R_p(\phi)}{\partial \theta} M_\theta(\phi, \theta) \\
 &\quad - R_0 R_p(\phi) Q_\phi(\phi, \theta) - R_p(\phi) (2I_3(\phi) \ddot{U}_0(\phi, \theta, t) + R_0(\phi) I_3(\phi) \ddot{\Psi}_\phi(\phi, \theta, t)) = 0, \\
 &R_0 \frac{\partial M_\theta(\phi, \theta)}{\partial \theta} + \frac{dR_p(\phi)}{d\phi} M_{\phi\theta}(\phi, \theta) + R_p(\phi) \frac{\partial M_{\phi\theta}(\phi, \theta)}{\partial \phi} + \frac{\partial R_p(\phi)}{\partial \phi} M_{\theta\phi}(\phi, \theta) \\
 &\quad - R_0 R_p(\phi) Q_\theta(\phi, \theta) - R_p(\phi) (2I_3(\phi) V_0(\phi, \theta, t) + R_0 I_3(\phi) \ddot{\Psi}_\theta(\phi, \theta, t)) = 0.
 \end{aligned} \right\} \tag{4}$$

with variable quantities  $I_1(\phi), I_3(\phi)$  obtained by integration of the material density through the thickness as follows:

$$I_1(\phi) = \int_{-h(\phi)/2}^{+h(\phi)/2} \rho dz = \rho h(\phi), \quad I_3(\phi) = \int_{-h(\phi)/2}^{+h(\phi)/2} \rho z^2 dz = \frac{\rho h^3(\phi)}{12}. \tag{5}$$

The stress-strain relations for an isotropic material are given by

$$\begin{Bmatrix} \sigma_\phi \\ \sigma_\theta \\ \sigma_{\phi\theta} \\ \sigma_{\phi z} \\ \sigma_{\theta z} \end{Bmatrix} = \frac{E}{1-\mu^2} \begin{bmatrix} 1 & \mu & 0 & 0 & 0 \\ \mu & 1 & 0 & 0 & 0 \\ 0 & 0 & (1-\mu)/2 & 0 & 0 \\ 0 & 0 & 0 & (1-\mu)/2 & 0 \\ 0 & 0 & 0 & 0 & (1-\mu)/2 \end{bmatrix} \begin{Bmatrix} \epsilon_\phi \\ \epsilon_\theta \\ \gamma_{\phi\theta} \\ \gamma_{\phi z} \\ \gamma_{\theta z} \end{Bmatrix}, \quad (6)$$

where  $E$  is the modulus of elasticity and  $\mu$  is Poisson's ratio. For isotropic materials the force and moment resultants are obtained by integrating the stresses through the shell thickness, which in this case is variable along the meridian:

$$\begin{Bmatrix} N_\phi(\phi, \theta) \\ N_\theta(\phi, \theta) \\ N_{\phi\theta}(\phi, \theta) \\ N_{\theta\phi}(\phi, \theta) \end{Bmatrix} = \int_{-h(\phi)/2}^{+h(\phi)/2} \begin{Bmatrix} \sigma_\phi(z) \\ \sigma_\theta(z) \\ \sigma_{\phi\theta}(z) \\ \sigma_{\theta\phi}(z) \end{Bmatrix} \left(1 + \frac{z}{R_0}\right) dz, \quad (7)$$

$$\begin{Bmatrix} Q_\phi(\phi, \theta) \\ Q_\theta(\phi, \theta) \end{Bmatrix} = \kappa \int_{-h(\phi)/2}^{+h(\phi)/2} \begin{Bmatrix} \sigma_{\phi z}(z) \\ \sigma_{\theta z}(z) \end{Bmatrix} \left(1 + \frac{z}{R_0}\right) dz, \quad (8)$$

$$\begin{Bmatrix} M_\phi(\phi, \theta) \\ M_\theta(\phi, \theta) \\ M_{\phi\theta}(\phi, \theta) \\ M_{\theta\phi}(\phi, \theta) \end{Bmatrix} = \int_{-h(\phi)/2}^{+h(\phi)/2} \begin{Bmatrix} \sigma_\phi(z) \\ \sigma_\theta(z) \\ \sigma_{\phi\theta}(z) \\ \sigma_{\theta\phi}(z) \end{Bmatrix} \left(1 + \frac{z}{R_0}\right) z dz, \quad (9)$$

where  $\kappa$  is a shear correction factor. Various derivations of the shear correction factor have been proposed. [Mindlin \[1951\]](#) gave an implicit result for the shear correction factor for isotropic elastic plates that depends on Poisson ratio  $\mu$ . [Hutchinson \[1984\]](#) determined the shear coefficient in a Mindlin plate equation based on matching a mode of the Mindlin plate theory to the exact Rayleigh–Lamb frequency equation for the flexural wave response at long wavelengths and proposed the value  $\kappa = 5/(6 - \mu)$ . Later, [Stephen \[1997\]](#) reexamined this solution, and called this the “best” shear coefficient. In the present work this value of Hutchinson's shear coefficient is used in the calculations.

Considering the stress-strain relations, the kinematical relations for shells with variable thickness the constitutive relations become

$$\begin{aligned} N_\phi(\phi, \theta) &= \frac{E}{1-\mu^2} h(\phi) (\epsilon_{0\phi} + \mu \epsilon_{0\theta}), & N_\theta(\phi, \theta) &= \frac{E}{1-\mu^2} h(\phi) (\mu \epsilon_{0\phi} + \epsilon_{0\theta}), \\ Q_\phi(\phi, \theta) &= \frac{\kappa E}{2(1+\mu)} h(\phi) \gamma_{0\phi n}, & Q_\theta(\phi, \theta) &= \frac{\kappa E}{2(1+\mu)} h(\phi) \gamma_{0\theta n}, \\ N_{\phi\theta}(\phi, \theta) &= \frac{E}{2(1+\mu)} h(\phi) (\gamma_{0\phi\theta} + \gamma_{0\theta\phi}), & N_{\theta\phi}(\phi, \theta) &= N_{\phi\theta}(\phi, \theta), \\ M_\phi(\phi, \theta) &= \frac{E}{1-\mu^2} \frac{h^3(\phi)}{12} (k_\phi + \mu k_\theta), & M_\theta(\phi, \theta) &= \frac{E}{1-\mu^2} \frac{h^3(\phi)}{12} (\mu k_\phi + k_\theta), \\ M_{\phi\theta}(\phi, \theta) &= \frac{E}{2(1+\mu)} \frac{h^3(\phi)}{12} (\tau_{\phi\theta} + \tau_{\theta\phi}), & M_{\theta\phi}(\phi, \theta) &= M_{\phi\theta}(\phi, \theta). \end{aligned} \quad (10)$$

### 3. Solution procedure

We introduce a nondimensional coordinate  $\xi = (\phi - \phi_b)/\phi_0$  that vary from 0 to 1. The variation of the geometric parameters  $h$  and  $R_p$  is taken in a polynomial form as follows:

$$h(\phi) \implies h(\xi) = \sum_{i=0}^{nh} h_i \xi^i, \quad R_p(\phi) \implies R_p(\xi) = \sum_{i=0}^{nR_p} R_{pi} \xi^i, \quad (11)$$

Spherical shell segments with a wide range of meridian opening angles, concave or convex thickness variation can be described in this way, up to any desired accuracy. In case of shell with wavy or corrugated surface, it could be represented by segmented shell with sequential shell segments with convex and concave thickness variation.

When the force and moment resultants are substituted into the equations of motion (4), assuming harmonic vibrations, and using the assumed displacement field

$$\begin{aligned} U_0(\phi, \theta, t) &= u(\phi) \cos n\theta \sin \omega t, \\ V_0(\phi, \theta, t) &= v(\phi) \sin n\theta \sin \omega t, \\ W_0(\phi, \theta, t) &= w(\phi) \cos n\theta \sin \omega t, \\ \Psi_\phi(\phi, \theta, t) &= \psi_\phi(\phi) \cos n\theta \sin \omega t, \\ \Psi_\theta(\phi, \theta, t) &= \psi_\theta(\phi) \sin n\theta \sin \omega t, \end{aligned} \quad (12)$$

with the notation

$$U(\phi) = \{u(\phi), v(\phi), w(\phi), \psi_\phi(\phi), \psi_\theta(\phi)\}^T \quad (13)$$

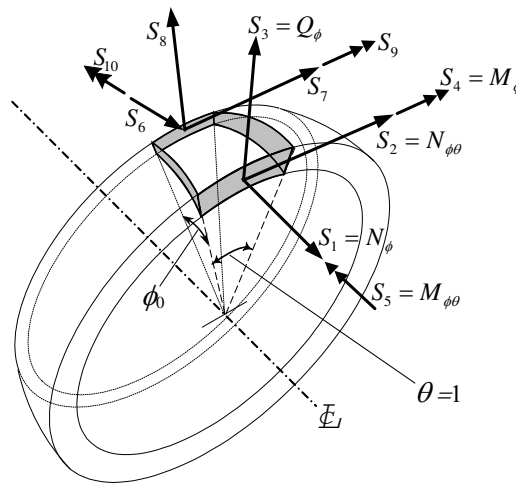


**Figure 2.** Dynamic stiffnesses defined by resultant forces along a unit angle segment of the perimeter of the shell edges ( $\xi = 0, \xi = 1$ ).

after transformation to the nondimensional coordinate  $\xi$ , we obtain the equations of motion in term of the displacements as

$$\mathbf{K}^{(0)}(\xi, \omega)\mathbf{U}(\xi) + \mathbf{K}^{(1)}(\xi)\mathbf{U}'(\xi) + \mathbf{K}^{(2)}(\xi)\mathbf{U}''(\xi) = 0, \quad (14)$$

where primes refer to derivatives with respect to  $\xi$ , and the terms in the matrices  $\mathbf{K}^{(0)}$ ,  $\mathbf{K}^{(1)}$ , and  $\mathbf{K}^{(2)}$  are given in the [Appendix](#). The solution is obtained using the exact element method algorithm [[Eisenberger 1990](#)] by assuming the solution as infinite power series

$$\mathbf{U}(\xi) = \sum_{i=0}^{\infty} \mathbf{u}_i \xi^i, \quad (15)$$

and following the procedure in [[Eisenberger 1990](#)] we get the five basic shape functions for each case of unit displacement on the shell edges. Based on the values of the shape functions and their derivatives at the two edges of the segment ( $\xi = 0$ ;  $\xi = 1$ ) we get the terms in the dynamic stiffness matrix as the resultant forces along the unit angle segment of the perimeter of the shell, as shown in [Figure 2](#), as

$$\begin{aligned} \left. \begin{matrix} S_1 \\ S_6 \end{matrix} \right\} &= N_\phi \bigg|_{\substack{\xi=0 \\ \xi=1}} = \frac{E}{1-\mu^2} \left[ \frac{R'_p \Phi}{R_0} \mu u + \frac{R_p \Phi}{R_0} u' + \mu n v + \left( \frac{R_p}{R_0} (1+\mu) \right) w \right] \bigg|_{\substack{\xi=0 \\ \xi=1}}, \\ \left. \begin{matrix} S_2 \\ S_7 \end{matrix} \right\} &= N_{\phi\theta} \bigg|_{\substack{\xi=0 \\ \xi=1}} = \frac{E}{2(1+\mu)} \left[ -nu - \frac{R'_p \Phi}{R_0} v + \frac{R_p \Phi}{R_0} v' \right] \bigg|_{\substack{\xi=0 \\ \xi=1}}, \\ \left. \begin{matrix} S_3 \\ S_8 \end{matrix} \right\} &= Q_\phi \bigg|_{\substack{\xi=0 \\ \xi=1}} = \frac{\kappa E}{2(1+\mu)} \left[ -\frac{R_p}{R_0} u + \frac{R_p \Phi}{R_0} w' + \psi_s \right] \bigg|_{\substack{\xi=0 \\ \xi=1}}, \\ \left. \begin{matrix} S_4 \\ S_9 \end{matrix} \right\} &= M_\phi \bigg|_{\substack{\xi=0 \\ \xi=1}} = \frac{E}{(1-\mu^2)} \frac{h^3}{12} \left[ \mu \frac{R'_p \Phi}{R_0} \psi_\phi + \frac{R_p \Phi}{R_0} \psi'_\phi + \mu n \psi_\phi \right] \bigg|_{\substack{\xi=0 \\ \xi=1}}, \\ \left. \begin{matrix} S_5 \\ S_{10} \end{matrix} \right\} &= M_{\phi\theta} \bigg|_{\substack{\xi=0 \\ \xi=1}} = \frac{E}{2(1+\mu)} \frac{h^3}{12} \left[ -n \psi_\phi - \frac{R'_p \Phi}{R_0} \psi_\theta + \left( \frac{R_p}{R_0} \right) \Phi \psi'_\theta \right] \bigg|_{\substack{\xi=0 \\ \xi=1}}. \end{aligned} \quad (16)$$

The dynamic stiffness matrix for a segment, having ten degrees of freedom, five on each edge, is then assembled for the structure in the usual procedure of structural analysis. The natural frequencies of vibration are found as the values of the frequency that will cause the assembled dynamic stiffness matrix of the structure to become singular.

When the cut-outs size becomes relatively small ( $R_{p,\text{in}}/R_{p,\text{out}} < 0.1$ ) the shape functions series converges rather slowly and have relatively large number of terms. Therefore, in order speed the convergence process one can divide the shell into sections with ratio  $R_{p,\text{in}} = 0.3R_{p,\text{out}}$  for each section. So, by adding a small number of elements one can solve for shells with very small cut-outs (e.g., three elements for  $R_{p,\text{in}} = 0.03R_{p,\text{out}}$  and four elements for  $R_{p,\text{in}} = 0.01R_{p,\text{out}}$ ).

#### 4. Numerical examples

In order to obtain a high-precision solution for vibration problems of thick spherical shells, numerical calculations have been performed for a spherical shells with different thickness-radius ratios, and various

| <i>n</i> | <i>h/R</i> = 0.1 |              |              |         |       |        | <i>h/R</i> = 0.2 |       |        |         |       |        |
|----------|------------------|--------------|--------------|---------|-------|--------|------------------|-------|--------|---------|-------|--------|
|          | Clamped-Free     |              |              | SS-Free |       |        | Clamped-Free     |       |        | SS-Free |       |        |
|          | 5 DOF            | Lit.         | Diff.%       | 7 DOF   | Lit.  | Diff.% | 5 DOF            | Lit.  | Diff.% | 7 DOF   | Lit.  | Diff.% |
| 0        | 0.9810           | 0.978        | 0.30         | 0.9079  | 0.906 | 0.21   | 1.1403           | 1.133 | 0.64   | 1.0516  | 1.047 | 0.44   |
|          | 1.3025           | 1.297        | 0.42         | 1.3025  | 1.297 | 0.42   | 1.3025           | 1.297 | 0.42   | 1.3022  | 1.297 | 0.40   |
|          | 1.3398           | 1.340        | -0.01        | 1.3398  | 1.340 | -0.02  | 1.4212           | 1.427 | -0.40  | 1.3583  | 1.358 | 0.02   |
| 1        | 0.7052           | 0.704        | 0.17         | 0.6593  | 0.658 | 0.19   | 0.7553           | 0.753 | 0.30   | 0.6785  | 0.678 | 0.08   |
|          | 1.0757           | 1.073        | 0.25         | 1.0172  | 1.014 | 0.32   | 1.2999           | 1.295 | 0.38   | 1.2065  | 1.203 | 0.29   |
|          | 1.6828           | 1.684        | -0.07        | 1.5745  | 1.572 | 0.16   | 1.9858           | 1.982 | 0.19   | 1.9829  | 1.965 | 0.91   |
| 2        | 0.4477           | 0.445        | 0.61         | 0.4111  | 0.409 | 0.51   | 0.6530           | 0.653 | 0.00   | 0.5687  | 0.571 | -0.41  |
|          | 1.2783           | 1.275        | 0.26         | 1.1921  | 1.185 | 0.60   | 1.6917           | 1.688 | 0.22   | 1.5586  | 1.550 | 0.56   |
|          | 1.8342           | 1.835        | -0.05        | 1.7248  | 1.722 | 0.16   | 2.0241           | 2.022 | 0.10   | 2.0181  | 2.007 | 0.55   |
| 3        | 0.7617           | 0.764        | -0.30        | 0.7453  | 0.747 | -0.23  | 1.1415           | 1.157 | -1.34  | 1.0726  | 1.086 | -1.24  |
|          | 1.4676           | 1.465        | 0.17         | 1.3656  | 1.357 | 0.63   | 2.0931           | 2.087 | 0.29   | 1.9374  | 1.922 | 0.80   |
|          | 2.1411           | 2.142        | -0.04        | 1.9834  | 1.979 | 0.22   | 2.4381           | 2.435 | 0.13   | 2.4306  | 2.428 | 0.11   |
| 4        | 1.1698           | 1.176        | -0.52        | 1.1406  | 1.145 | -0.38  | 1.6949           | 1.719 | -1.40  | 1.6041  | 1.622 | -1.11  |
|          | 1.7184           | 1.718        | 0.02         | 1.6085  | 1.602 | 0.41   | 2.5572           | 2.557 | 0.01   | 2.4219  | 2.426 | -0.17  |
|          | 2.4824           | <b>2.776</b> | <b>-10.6</b> | 2.3148  | 2.311 | 0.17   | 3.1124           | 3.107 | 0.17   | 3.0877  | 3.087 | 0.02   |
| 5        | 1.5177           | 1.525        | -0.48        | 1.4576  | 1.461 | -0.23  | 2.2095           | 2.235 | -1.14  | 2.0996  | 2.118 | -0.87  |
|          | 2.1060           | 2.109        | -0.14        | 1.9964  | 1.994 | 0.12   | 3.1445           | 3.151 | -0.21  | 3.0215  | 3.024 | -0.08  |
|          | 2.8804           | 2.885        | -0.16        | 2.7240  | 2.721 | 0.11   | 3.8489           | 3.860 | -0.29  | 3.8133  | 3.851 | -0.98  |

**Table 1.** Nondimensional frequency  $\lambda = \omega R \sqrt{\rho/E}$  for a hemispherical shell with a 30° cutout at the apex, with free boundary conditions at the cutout and different boundary conditions at the base. The columns “5 DOF” and “7 DOF” give the result with the present method (one exact element and the specified number of degrees of freedom). “Lit.” refers to [Gautham and Ganesan 1992]. “Diff.%” is the ratio  $(\lambda_{\text{exact}} - \lambda_{\text{FE}})/\lambda_{\text{FE}}$ .

combinations of boundary conditions: constant thickness hemispherical caps with annular cutout at the apex, variable thickness spherical annular segment, and variable thickness spherical barrel shell.

The results for the constant thickness hemispherical shells are set out in Tables 1 and 2 for two cutout sizes (60° and 30°), and with two types of boundary conditions at the base: clamped and simply supported, and two thickness/radius ratios: 0.1 and 0.2. A comparison is made with the results of the FE analysis of [Gautham and Ganesan 1992] that were obtained by using Nagdhi’s basic relations that take the transverse shear and the normal strain into consideration. Three-noded finite elements with 7 DOF per node were used for solving the problem. Good general agreement of the results is shown. Some fictitious frequencies given by FE analysis can be observed (marked in bold).

Table 3, left, presents a comparison of the natural frequencies for an annular hemispherical shell with linearly varying thickness ( $\phi_0 = 60^\circ$ ,  $h_b/h_e = 1/3$ ) (Figure 3, left). The comparison is performed with the results from FE analysis using the commercial code ABAQUS, and the results from a three-dimensional analysis by the Ritz method reported in [Kang and Leissa 2006]. The results of the present

| $n$ | $h/R = 0.1$  |       |        |         |              |              | $h/R = 0.2$  |       |        |         |       |        |
|-----|--------------|-------|--------|---------|--------------|--------------|--------------|-------|--------|---------|-------|--------|
|     | Clamped-Free |       |        | SS-Free |              |              | Clamped-Free |       |        | SS-Free |       |        |
|     | 5 DOF        | Lit.  | Diff.% | 7 DOF   | Lit.         | Diff.%       | 5 DOF        | Lit.  | Diff.% | 7 DOF   | Lit.  | Diff.% |
| 0   | 1.1353       | 1.139 | -0.32  | 1.0722  | 1.072        | 0.02         | 1.2777       | 1.289 | -0.88  | 1.0583  | 1.059 | -0.06  |
|     | 2.0232       | 2.014 | 0.45   | 1.7280  | 1.726        | 0.12         | 2.0232       | 2.013 | 0.50   | 2.0223  | 2.014 | 0.41   |
|     | 2.1232       | 2.125 | -0.08  | 2.0231  | 2.010        | 0.65         | 2.7504       | 2.747 | 0.12   | 2.4947  | 2.487 | 0.31   |
| 1   | 0.9833       | 0.984 | -0.07  | 0.8890  | 0.887        | 0.22         | 1.1492       | 1.152 | -0.24  | 0.8968  | 0.895 | 0.20   |
|     | 2.1026       | 2.106 | -0.16  | 1.7584  | 1.756        | 0.14         | 2.3395       | 2.337 | 0.11   | 2.3347  | 2.332 | 0.12   |
|     | 2.4140       | 2.408 | 0.25   | 2.3790  | 2.369        | 0.42         | 2.8142       | 2.810 | 0.15   | 2.5781  | 2.565 | 0.51   |
| 2   | 0.7965       | 0.794 | 0.32   | 0.6507  | 0.648        | 0.41         | 1.0567       | 1.053 | 0.35   | 0.7540  | 0.751 | 0.40   |
|     | 2.2267       | 2.232 | -0.24  | 1.8775  | <b>2.038</b> | <b>-7.88</b> | 2.8075       | 2.822 | -0.51  | 2.6616  | 2.670 | -0.31  |
|     | 3.0967       | 3.088 | 0.28   | 3.0846  | <b>2.764</b> | <b>11.6</b>  | 3.1626       | 3.150 | 0.40   | 3.1131  | 3.087 | 0.85   |
| 3   | 0.7515       | 0.748 | 0.47   | 0.5844  | 0.581        | 0.58         | 1.1578       | 1.154 | 0.33   | 0.8790  | 0.879 | 0.00   |
|     | 2.4119       | 2.416 | -0.17  | 2.0644  | <b>2.522</b> | <b>-18.1</b> | 3.0761       | 3.099 | -0.74  | 2.9268  | 2.939 | -0.42  |
|     | 3.3919       | 3.398 | -0.18  | 3.3843  | <b>2.524</b> | <b>34.1</b>  | 3.6591       | 3.634 | 0.69   | 3.5337  | 3.459 | 2.16   |
| 4   | 0.8764       | 0.873 | 0.39   | 0.7344  | 0.731        | 0.47         | 1.4400       | 1.441 | -0.07  | 1.2250  | 1.230 | -0.40  |
|     | 2.6411       | 2.643 | -0.07  | 2.2964  | 2.307        | -0.46        | 3.3779       | 3.407 | -0.85  | 3.2616  | 3.278 | -0.50  |
|     | 3.5287       | 3.532 | -0.09  | 3.5250  | 3.477        | 1.38         | 3.8222       | 3.782 | 1.06   | 3.6590  | 3.586 | 2.03   |
| 5   | 1.1272       | 1.126 | 0.11   | 1.0160  | 1.014        | 0.20         | 1.8473       | 1.853 | -0.31  | 1.6855  | 1.693 | -0.44  |
|     | 2.8959       | 2.894 | 0.06   | 2.5589  | 2.546        | 0.51         | 3.7419       | 3.772 | -0.80  | 3.6600  | 3.675 | -0.41  |
|     | 3.7873       | 3.789 | -0.04  | 3.7869  | 3.780        | 0.18         | 4.0686       | 4.025 | 1.08   | 3.8853  | 3.818 | 1.76   |

**Table 2.** Nondimensional frequency  $\lambda = \omega R \sqrt{\rho/E}$  for hemispherical shells with  $60^\circ$  cutout at the apex, with free boundary conditions at the cutout and different boundary conditions at the base. The columns “5 DOF” and “7 DOF” give the result with the present method (one exact element and the specified number of degrees of freedom). “Lit.” refers to [Gautham and Ganesan 1992]. “Diff.%” is the ratio  $(\lambda_{\text{exact}} - \lambda_{\text{FE}})/\lambda_{\text{FE}}$ .

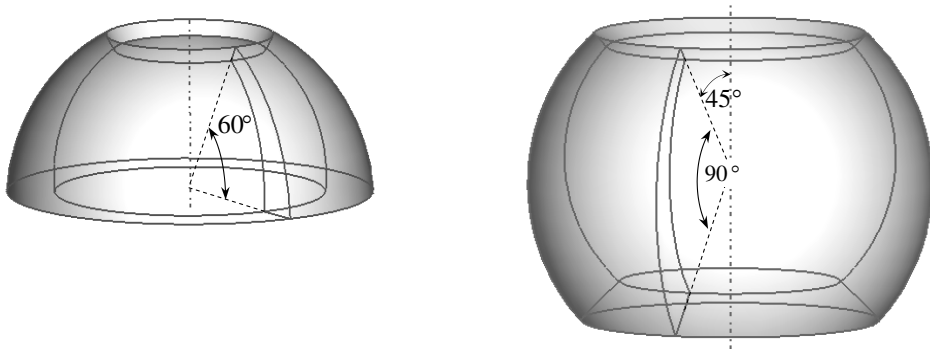


**Figure 3.** Left: hemispherical annular shell with linearly varying thickness;  $\phi_0 = 60^\circ$ ,  $h_b/h_e = 1/3$  (results in Table 3, left). Right: spherical barrel shell with variable thickness;  $\phi_b = 45^\circ$ ,  $\phi_e = 135^\circ$ ,  $(h_b + h_e)/2R = 0.2$ ,  $h_b/h_e = 1/3$ ,  $\mu = 0.3$  (results in Table 3, right, and Figures 4–7).

| $n$   | 2D FE<br>1600 S4R<br>shell els.<br>10080 DOF | 3D FE<br>2095 C3D20R<br>solid els.<br>43020 DOF | [Kang and<br>Leissa<br>2006]<br>3D, Ritz | Present<br>DSM with<br>2 exact els.<br>15 DOF | 3D FE<br>2095 C3D20R<br>solid els.<br>43020 DOF | [Kang and<br>Leissa<br>2006]<br>3D, Ritz | Present<br>DSM with<br>3 exact els.<br>20 DOF |
|-------|--|---|--|---|---|--|---|
| 0 (A) | 1.5357                                       | 1.5361  | 1.536                                    | 1.5347  | 1.5345  | 1.535                                    | 1.5299  |
|       | 2.1152                                       | 2.0862  | 2.090                                    | 2.1138  | 1.9099  | 1.911                                    | 1.9268  |
|       | 2.3992                                       | 2.4216  | 2.423                                    | 2.4057  | 1.9632  | 1.963                                    | 1.9651  |
|       | 4.3117                                       | 4.3143  | 4.322                                    | 4.3041  | 2.4772  | 2.487                                    | 2.4846  |
|       | 5.9909                                       | 5.8511  | 5.844                                    | 5.9780  | 3.8292  | 3.844                                    | 3.8355  |
| 0 (T) | 3.7144                                       | 3.6775  | 3.669                                    | 3.7053  | 2.4774  | 2.470                                    | 2.4938  |
|       | 6.5151                                       | 6.3843  | 6.385                                    | 6.4586  | 4.2877  | 4.290                                    | 4.3343  |
|       | 9.5088                                       | 9.1976  | 9.200                                    | 9.3248  | 6.1689  | 6.172                                    | 6.2411  |
|       |  |   |  |   | NA  | 8.093                                    | 8.1862  |
| 1     | 1.5666                                       | 1.5687  | 1.568                                    | 1.5645  | 1.3915  | 1.390                                    | 1.3898  |
|       | 2.4016                                       | 2.3730  | 2.374                                    | 2.3990  | 1.7690  | 1.771                                    | 1.7688  |
|       | 2.4824                                       | 2.4819  | 2.485                                    | 2.4845  | 2.3793  | 2.379                                    | 2.4037  |
|       | 4.4149                                       | 4.4072  | 4.414                                    | 4.4101  | 2.5836  | 2.594                                    | 2.5915  |
|       | 4.6268                                       | 4.5782  | 4.572                                    | 4.6131  | 3.4497  | 3.445                                    | 3.4897  |
| 2     | 0.3495                                       | 0.3495  | 0.349                                    | 0.3494  | 0.3593  | 0.362                                    | 0.3613  |
|       | 0.7135                                       | 0.7031  | 0.705                                    | 0.7136  | 0.6065  | 0.604                                    | 0.6076  |
|       | 1.8514                                       | 1.8563  | 1.857                                    | 1.8443  | 1.6842  | 1.690                                    | 1.6977  |
|       | 2.8071                                       | 2.8044  | 2.809                                    | 2.8093  | 2.0238  | 2.027                                    | 2.0281  |
|       | 3.6503                                       | 3.5714  | 3.572                                    | 3.6372  | 2.8902  | 2.901                                    | 2.9006  |
| 3     | 0.9382                                       | 0.9368  | 0.934                                    | 0.9364  | 0.9085  | 0.918                                    | 0.9169  |
|       | 1.6815                                       | 1.6615  | 1.666                                    | 1.6794  | 1.4032  | 1.400                                    | 1.3997  |
|       | 2.6617                                       | 2.6422  | 2.646                                    | 2.6436  | 2.2845  | 2.298                                    | 2.3155  |
|       | 3.3486                                       | 3.3397  | 3.346                                    | 3.3494  | 2.6510  | 2.651                                    | 2.6687  |
|       | 4.8367                                       | 4.7495  | 4.746                                    | 4.8121  | 3.3737  | 3.385                                    | 3.3824  |
| 4     | 1.6823                                       | 1.6757  | 1.671                                    | 1.6753  | 1.5436  | 1.561                                    | 1.5597  |
|       | 2.6672                                       | 2.6368  | 2.643                                    | 2.6577  | 2.1947  | 2.196                                    | 2.1917  |
|       | 3.6246                                       | 3.5577  | 3.564                                    | 3.5878  | 2.9024  | 2.911                                    | 2.9192  |
|       | 4.0553                                       | 4.0540  | 4.060                                    | 4.0547  | 3.5713  | 3.579                                    | 3.6300  |
|       | 5.8216                                       | 5.8013  | 5.793                                    | 5.8063  | 4.0506  | 4.059                                    | 4.0507  |
| 5     | 2.5319                                       | 2.5140  | 2.507                                    | 2.5144  | 2.2465  | 2.271                                    | 2.2696  |
|       | 3.6775                                       | 3.6304  | 3.637                                    | 3.6558  | 2.9445  | 2.954                                    | 2.9478  |
|       | 4.5940                                       | 4.4686  | 4.475                                    | 4.5297  | 3.6991  | 3.707                                    | 3.7014  |
|       | 4.9368                                       | 4.9436  | 4.951                                    | 4.9250  | 4.4644  | 4.477                                    | 4.5276  |
|       | 6.6094                                       | 6.6536  | 6.665                                    | 6.6166  | 4.9457  | 4.952                                    | 4.9700  |

**Table 3.** Comparison of the nondimensional natural frequency  $\Omega = \omega R \sqrt{\rho/G}$  for completely free spherical shells with linearly varying thickness. Left: annular shell with  $\phi_b = 30^\circ$  and  $\phi_e = 90^\circ$  (Figure 3, left). Right: barrel shell with  $\phi_b = 45^\circ$  and  $\phi_e = 135^\circ$  (Figure 3, right). In both cases,  $(h_b + h_e)/2R = 0.2$ ,  $h_b/h_e = 1/3$ , and  $\mu = 0.3$ . “A” stands for axisymmetric modes, “T” for torsional modes.

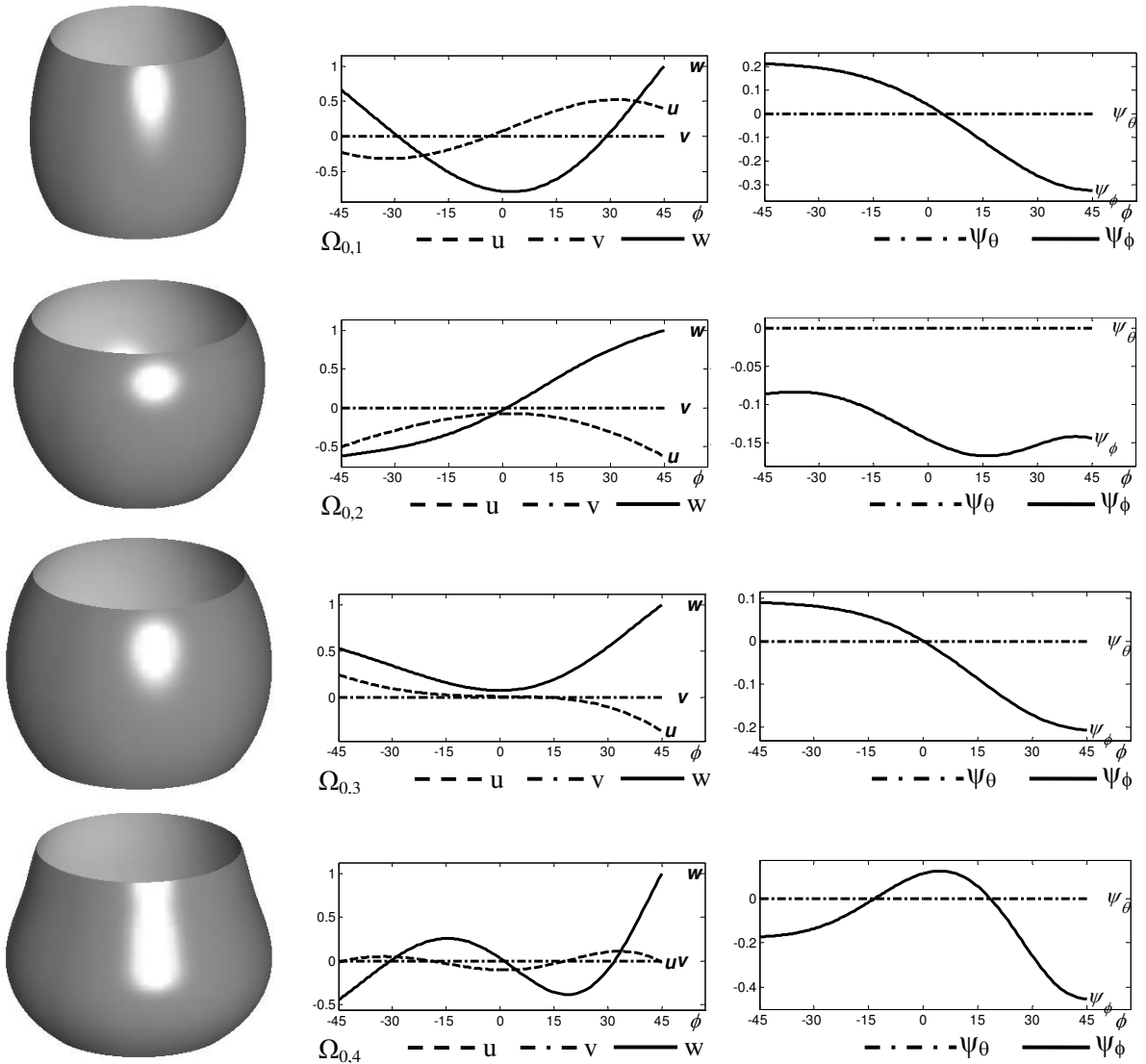


**Figure 4.** The first four mode shapes of axisymmetric vibrations ( $n = 0$ ) of completely free spherical barrel shell with variable thickness (Figure 3, right).

exact analysis are generally lower than the results from the two-dimensional FE analysis, and for some modes the frequency is a little bit higher due the difference in the shear correction factor that was used:  $5/(6 - \mu)$  in the present analysis versus  $5/6$  in the FE analysis. Comparison with the three-dimensional Ritz solution shows that the torsional modes in the present analysis are higher than the values in the three-dimensional analysis due to kinematical simplifications of the first order shear deformation shell theory. In other vibrational modes no clear tendency is observed.

The same conclusions are obtained from comparison of frequency results for barrel spherical shell ( $\phi_b = 45^\circ$ ,  $\phi_e = 135^\circ$ ,  $(h_b + h_e)/2R = 0.2$ ,  $h_b/h_e = 1/3$ ,  $\mu = 0.3$ ) presented in Table 3, right. Figures 4,

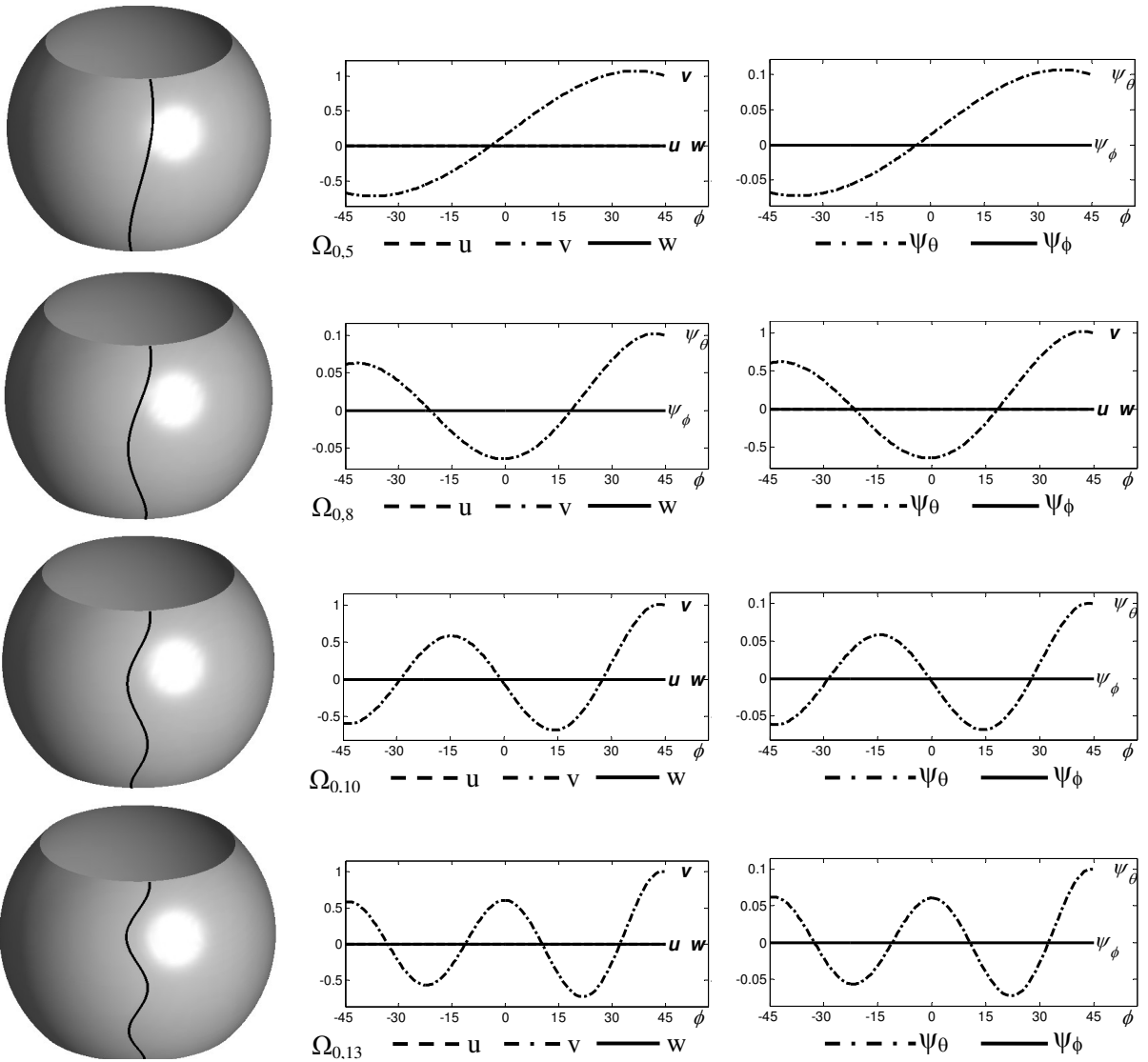


**Figure 5.** The first four mode shapes of pure torsional vibrations ( $n = 0$ ) of completely free spherical barrel shell with variable thickness (Figure 3, right).

5, 6, and 7 show the three-dimensional vibrational modes and the exact displacement shape functions obtained by the present method.

### 5. Conclusions

The natural frequencies for spherical shells of revolution with different boundary conditions have been investigated using the Dynamic Stiffness method. This approach is combined with the exact element method for the vibration analysis of spherical shell segments with curved meridian and variable cross-section. The analysis uses the equations of the two-dimensional theory of elasticity, in which the effects

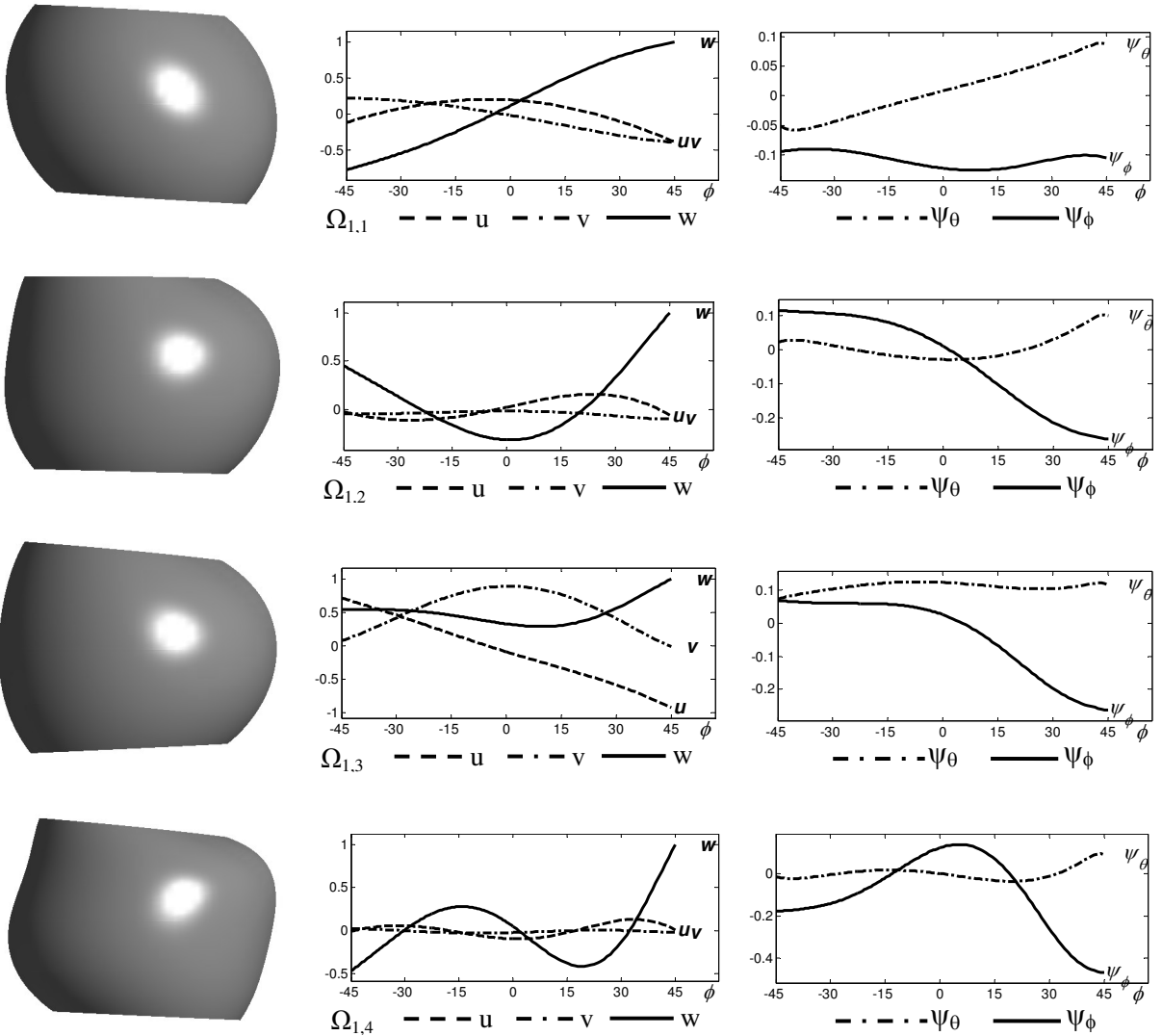


**Figure 6.** Mode shapes of vibrations with one circumferential waves ( $n = 1$ ) of a completely free spherical barrel shell with variable thickness (Figure 3, right).

of both transverse shear stresses and rotary inertia are accounted for, in their general forms for isotropic homogeneous materials. The proposed method shows the following advantages:

- (1) Any polynomial variation of the thickness of the shell along the meridian can be considered.
- (2) The method is mesh-free, and dividing the surface to many elements doesn't improve the solution. No convergence study is necessary to obtain the true results.
- (3) The shape functions are derived automatically and they are the exact solutions for the system of the differential equation of motion with variable coefficients. As a result, the solution for free vibrations

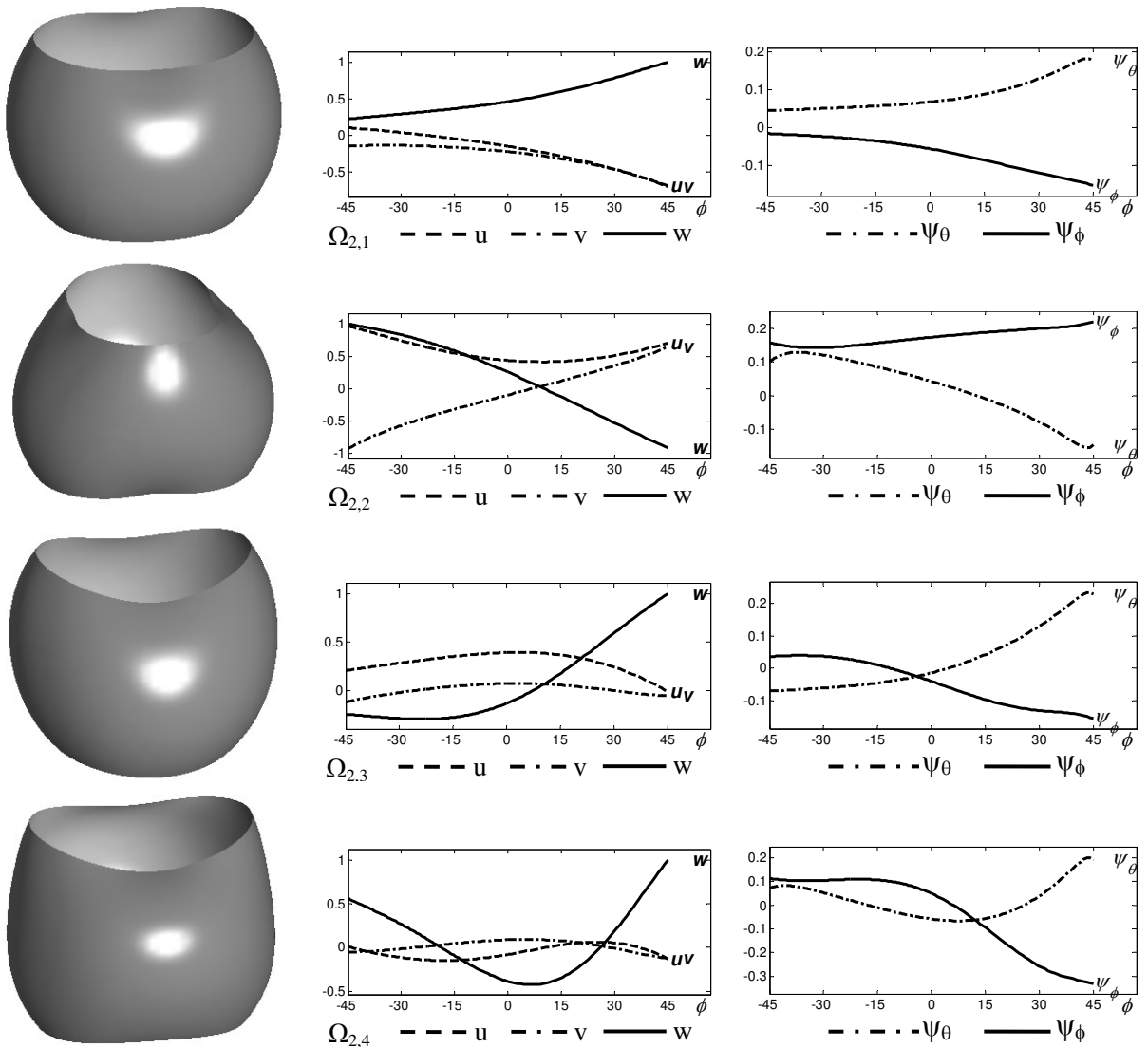


**Figure 7.** Mode shapes of vibrations with two circumferential waves ( $n = 2$ ) of a completely free spherical barrel shell with variable thickness (Figure 3, right).

problem is a highly accurate solution (depending only on the accuracy of the numerical calculations).

- (4) The order of the frequency determinants which are required for the solution by the present method are at least an order of magnitude smaller than those needed by a finite element analysis of comparable accuracy.
- (5) The derived dynamic stiffness matrix allows combination of spherical shell segments into complex assemblies with different combinations of shell types, variable thickness, and analyzing them with small number of elements.

**Appendix: Entries of the coefficient matrices  $K^{(0)}$ ,  $K^{(1)}$ , and  $K^{(2)}$  in Equation (14)**

Only nonzero entries are listed. We set  $\Phi = 1/\phi_0$ .

$$\begin{aligned}
 K_{11}^{(0)} &= \omega^2(\rho/E)(1-\mu^2)R_p^2R_0^3h + R_pR_0(R_p'h' + R_p''h)\Phi^2\mu - \frac{1}{2}(1-\mu)(R_p^2R_0\kappa h + R_0^3hn^2) \\
 K_{12}^{(0)} &= \frac{1}{2}R_0^2n\Phi R_p'h(\mu-3) + R_0^2n\Phi R_ph'\mu \\
 K_{13}^{(0)} &= R_p^2R_0h'\Phi(1+\mu) & K_{14}^{(0)} &= \frac{1}{6}\omega^2(\rho/E)(1-\mu^2)R_p^2R_0^2h^3 + \frac{1}{2}(1-\mu)R_p^2R_0^2\kappa h \\
 K_{21}^{(0)} &= \frac{1}{2}R_0^2n\Phi R_p'h(\mu-3) - \frac{1}{2}R_0^2n\Phi(1-\mu)R_ph' \\
 K_{22}^{(0)} &= \omega^2(1-\mu^2)(\rho/E)R_p^2R_0^3h - \frac{1}{2}(1-\mu)R_pR_p''R_0h\Phi^2\mu - \frac{1}{2}(1-\mu)R_pR_p'R_0h'\Phi^2 - R_0^3hn^2 \\
 &\quad - \frac{1}{2}(1-\mu)R_p^2R_0\kappa h - \frac{1}{2}(1-\mu)R_p^2R_0h\Phi^2 \\
 K_{23}^{(0)} &= -(1+\mu)R_pR_0^2hn - \frac{1}{2}(1-\mu)R_pR_0^2\kappa hn & K_{25}^{(0)} &= \frac{1}{6}\omega^2(\rho/E)(1-\mu^2)R_p^2R_0^2h^3 + \frac{1}{2}(1-\mu)R_p^2R_0^2\kappa h \\
 K_{31}^{(0)} &= -(1+\mu)R_pR_p'R_0\Phi h - \frac{1}{2}(1-\mu)R_pR_p'R_0\kappa h\Phi - \frac{1}{2}(1-\mu)R_p^2R_0\kappa h'\Phi \\
 K_{32}^{(0)} &= K_{23}^{(0)} & K_{33}^{(0)} &= \omega^2(\rho/E)(1-\mu^2)R_p^2R_0^3h - \frac{1}{2}(1-\mu)R_0^3\kappa hn^2 - 2(1+\mu)R_p^2R_0h \\
 K_{34}^{(0)} &= \frac{1}{2}(1-\mu)(R_p^2R_0^2\kappa h' + R_pR_p'R_0^2\Phi\kappa h) & K_{35}^{(0)} &= \frac{1}{2}(1-\mu)R_pR_0^3\kappa hn \\
 K_{41}^{(0)} &= K_{14}^{(0)} \\
 K_{44}^{(0)} &= \frac{1}{12}\omega^2(\rho/E)(1-\mu^2)R_p^2R_0^3h^3 - \frac{1}{24}(1-\mu)R_0^3h^3n^2 - \frac{1}{12}R_p^2R_0h^3\Phi^2(1+\mu) \\
 &\quad - \frac{1}{2}(1-\mu)R_p^2R_0^3\kappa h + \frac{1}{12}R_pR_p''R_0h^3\Phi^2\mu + \frac{1}{4}R_pR_p'R_0h'h^2\Phi^2\mu \\
 K_{45}^{(0)} &= \frac{1}{4}n\mu R_pR_0^2h'h^2\Phi - \frac{1}{24}R_p'R_0^2n\Phi h^3(3-\mu) \\
 K_{52}^{(0)} &= K_{25}^{(0)} & K_{53}^{(0)} &= K_{35}^{(0)} & K_{54}^{(0)} &= -\frac{1}{8}(1-\mu)nR_pR_0^2h'h^2\Phi - \frac{1}{24}R_p'R_0^2n\Phi h^3(3-\mu) \\
 K_{55}^{(0)} &= \frac{1}{12}\omega^2(\rho/E)(1-\mu^2)R_p^2R_0^3h^3 + \frac{1}{24}(1-\mu)R_pR_p''R_0h^3\Phi^2 + \frac{1}{8}(1-\mu)R_pR_p'R_0h'h^2\Phi^2\mu \\
 &\quad - \frac{1}{2}(1-\mu)R_p^2R_0^3\kappa h - \frac{1}{12}R_0^3n^2h^3 - \frac{1}{12}R_p^2R_0h^3\Phi^2(1-\mu) \\
 \\
 K_{11}^{(1)} &= R_pR_p'R_0h\Phi^2 + R_p^2R_0h'\Phi^2 \\
 K_{12}^{(1)} &= \frac{1}{2}(1+\mu)R_pR_0^2hn\Phi & K_{13}^{(1)} &= (1+\mu)R_p^2R_0\Phi h + \frac{1}{2}(1-\mu)R_p^2R_0K\Phi h \\
 K_{21}^{(1)} &= -K_{12}^{(1)} & K_{22}^{(1)} &= \frac{1}{2}(1-\mu)R_pR_p'R_0h\Phi^2 + \frac{1}{2}(1-\mu)R_p^2R_0h'\Phi^2 \\
 K_{31}^{(1)} &= -K_{13}^{(1)} \\
 K_{33}^{(1)} &= \frac{1}{2}(1-\mu)(R_p^2R_0\kappa h'\Phi^2 + R_pR_p'R_0^2\Phi^2\kappa h) & K_{34}^{(1)} &= \frac{1}{2}(1-\mu)R_p^2R_0^2\kappa h\Phi \\
 K_{43}^{(1)} &= K_{34}^{(1)} \\
 K_{44}^{(1)} &= \Phi^2R_0\left(\frac{1}{12}R_pR_p'h^3 + \frac{1}{4}R_p^2h'h^2\right) & K_{45}^{(1)} &= \frac{1}{24}(1+\mu)R_pR_0^2\Phi h^3n \\
 K_{54}^{(1)} &= -K_{45}^{(1)} & K_{55}^{(1)} &= \frac{1}{8}(1-\mu)2\Phi^2R_p^2R_0h'h^2 + \frac{1}{24}(1-\mu)R_pR_p'R_0h^3\Phi^2
 \end{aligned}$$

$$\begin{aligned}
K_{11}^{(2)} &= R_p^2 R_0 h \Phi^2 \\
K_{22}^{(2)} &= \frac{1}{2}(1 - \mu) R_p^2 R_0 h \Phi^2 \\
K_{33}^{(2)} &= \frac{1}{2}(1 - \mu) R_p^2 R_0 \kappa h \Phi^2 \\
K_{44}^{(2)} &= \frac{1}{12} R_p^2 R_0 \Phi^2 h^3 \\
K_{55}^{(2)} &= \frac{1}{24}(1 - \mu) R_p^2 R_0 \Phi^2 h^3
\end{aligned}$$

### References

- [Eisenberger 1990] M. Eisenberger, “An exact element method”, *Int. J. Numer. Methods Eng.* **30** (1990), 363–370.
- [Gautham and Ganesan 1992] B. P. Gautham and N. Ganesan, “Free vibration analysis of thick spherical shells”, *Comput. Struct.* **2**:45 (1992), 307–313.
- [Hutchinson 1984] J. R. Hutchinson, “Vibrations of thick free circular plates, exact versus approximate solutions”, *J. Appl. Mech. (ASME)* **51** (1984), 581–585.
- [Kang and Leissa 2000] J. H. Kang and A. W. Leissa, “Three-dimensional vibrations of thick spherical shell segments with variable thickness”, *Int. J. Solids Struct.* **37** (2000), 4811–4823.
- [Kang and Leissa 2006] J. H. Kang and A. W. Leissa, “Corrigendum to Three-dimensional vibrations of thick spherical shell segments with variable thickness”, *Int. J. Solids Struct.* **43** (2006), 2848–2851.
- [Leissa 1973] A. W. Leissa, *Vibrations of shells*, US Government Printing Office, 1973. Reprinted Acoustical Soc. Amer., New York, 1993.
- [Leissa and Chang 1996] A. W. Leissa and J. D. Chang, “Elastic deformation of thick, laminated composite shells”, *Compos. Struct.* **35** (1996), 153–170.
- [Lim et al. 1996] C. W. Lim, S. Kitipornchai, and K. M. Liew, “Modeling the vibration of a variable thickness ellipsoidal dish with central point clamp or concentric surface clamp”, *J. Acoust. Soc. Am.* **1**:99 (1996), 362–372.
- [Mindlin 1951] R. D. Mindlin, “Influence of rotatory inertia and shear on flexural motions of isotropic, elastic plates”, *J. Appl. Mech. (ASME)* **18** (1951), 31–38.
- [Qatu 2002] M. S. Qatu, “Recent research advances in the dynamic behavior of shells: 1989–2000, Part 2: Homogeneous shells”, *Appl. Mech. Rev.* **5**:55 (2002), 415–434.
- [Stephen 1997] N. G. Stephen, “Mindlin plate theory: best shear coefficient and higher spectra validity”, *J. Sound Vib.* **202**:4 (1997), 539–553.

Received 3 Jan 2010. Revised 19 Apr 2010. Accepted 3 May 2010.

ELIA EFRAIM: [efraime@ariel.ac.il](mailto:efraime@ariel.ac.il)

Department of Civil Engineering, Ariel University Center of Samaria, 40700 Ariel, Israel

MOSHE EISENBERGER: [cvrmosh@technion.ac.il](mailto:cvrmosh@technion.ac.il)

Faculty of Civil and Environmental Engineering, Technion – Israel Institute of Technology, Technion City, 32000 Haifa, Israel

# JOURNAL OF MECHANICS OF MATERIALS AND STRUCTURES

<http://www.jomms.org>

Founded by Charles R. Steele and Marie-Louise Steele

## EDITORS

CHARLES R. STEELE Stanford University, U.S.A.  
DAVIDE BIGONI University of Trento, Italy  
IWONA JASIUK University of Illinois at Urbana-Champaign, U.S.A.  
YASUhide SHINDO Tohoku University, Japan

## EDITORIAL BOARD

H. D. BUI École Polytechnique, France  
J. P. CARTER University of Sydney, Australia  
R. M. CHRISTENSEN Stanford University, U.S.A.  
G. M. L. GLADWELL University of Waterloo, Canada  
D. H. HODGES Georgia Institute of Technology, U.S.A.  
J. HUTCHINSON Harvard University, U.S.A.  
C. HWU National Cheng Kung University, R.O. China  
B. L. KARIHALOO University of Wales, U.K.  
Y. Y. KIM Seoul National University, Republic of Korea  
Z. MROZ Academy of Science, Poland  
D. PAMPLONA Universidade Católica do Rio de Janeiro, Brazil  
M. B. RUBIN Technion, Haifa, Israel  
A. N. SHUPIKOV Ukrainian Academy of Sciences, Ukraine  
T. TARNAI University Budapest, Hungary  
F. Y. M. WAN University of California, Irvine, U.S.A.  
P. WRIGGERS Universität Hannover, Germany  
W. YANG Tsinghua University, P.R. China  
F. ZIEGLER Technische Universität Wien, Austria

## PRODUCTION

PAULO NEY DE SOUZA Production Manager  
SHEILA NEWBERY Senior Production Editor  
SILVIO LEVY Scientific Editor

Cover design: Alex Scorpan

Cover photo: Wikimedia Commons

See inside back cover or <http://www.jomms.org> for submission guidelines.

JoMMS (ISSN 1559-3959) is published in 10 issues a year. The subscription price for 2010 is US \$500/year for the electronic version, and \$660/year (+\$60 shipping outside the US) for print and electronic. Subscriptions, requests for back issues, and changes of address should be sent to Mathematical Sciences Publishers, Department of Mathematics, University of California, Berkeley, CA 94720-3840.

JoMMS peer-review and production is managed by EditFLOW™ from Mathematical Sciences Publishers.

PUBLISHED BY

 **mathematical sciences publishers**  
<http://www.mathscipub.org>

A NON-PROFIT CORPORATION

Typeset in L<sup>A</sup>T<sub>E</sub>X

©Copyright 2010. Journal of Mechanics of Materials and Structures. All rights reserved.

- Axial compression of hollow elastic spheres** ROBERT SHORTER, JOHN D. SMITH,  
VINCENT A. COVENEY and JAMES J. C. BUSFIELD 693
- Coupling of peridynamic theory and the finite element method**  
BAHATTIN KILIC and ERDOGAN MADENCI 707
- Genetic programming and orthogonal least squares: a hybrid approach to  
modeling the compressive strength of CFRP-confined concrete cylinders**  
AMIR HOSSEIN GANDOMI, AMIR HOSSEIN ALAVI, PARVIN ARJMANDI,  
ALIREZA AGHAEIFAR and REZA SEYEDNOUR 735
- Application of the Kirchhoff hypothesis to bending thin plates with different  
moduli in tension and compression** XIAO-TING HE, QIANG CHEN, JUN-YI  
SUN, ZHOU-LIAN ZHENG and SHAN-LIN CHEN 755
- A new modeling approach for planar beams: finite-element solutions based on  
mixed variational derivations**  
FERDINANDO AURICCHIO, GIUSEPPE BALDUZZI and CARLO LOVADINA 771
- SIFs of rectangular tensile sheets with symmetric double edge defects**  
XIANGQIAO YAN, BAOLIANG LIU and ZHAOHUI HU 795
- A nonlinear model of thermoelastic beams with voids, with applications**  
YING LI and CHANG-JUN CHENG 805
- Dynamic stiffness vibration analysis of thick spherical shell segments with variable  
thickness** ELIA EFRAIM and MOSHE EISENBERGER 821
- Application of a matrix operator method to the thermoviscoelastic analysis of  
composite structures** ANDREY V. PYATIGORETS, MIHAI O.  
MARASTEANU, LEV KHAZANOVICH and HENRYK K. STOLARSKI 837